Restart Strategy for Synchronous Reluctance Machine Driving a High Inertia Load

Kibok Lee, *IEEE Member,* Sara Ahmed and Srdjan M. Lukic, *IEEE Member*

***Abstract* — In many industrial settings, momentary power disruptions commonly occur, resulting in tripping of large electric machines, which then have to be brought to zero speed before the machine can be restarted. This approach can result in frequent interruptions in an industrial process, which can have negative effects on productivity. A more practical control implementation would restart the machine back to the original speed as soon as power is restored, not having to wait for the machine to be at a standstill. This concept is known as flying restart. In this paper we propose an approach to implement the universal restart for SynRM (Synchronous Reluctance Machine) through a simple identification algorithm which determines the speed and position of the machine so that the correct voltage vector can be applied and thus minimize the inrush current during the restart. The novelty of the proposed method is that its implementation only requires nameplate machine parameters and needs no machine-specific tuning, making the approach suitable for implementation with both high-inertia vector and scalar-controlled SynRM.**

***Index Terms*—Flying Restart, Synchronous Reluctance Motor (SynRM), Position and Speed Estimation.**

I. INTRODUCTION

In industrial setting, momentary power interruptions take place due to, for example, temporary power systems faults cleared by relay reclosing, with the interruption lasting as little as tens of milliseconds. In face of such interruptions, industrial machine controllers will typically need to restart from zero speed, implying that total shaft stoppage is required for the resumption of normal operation. This issue is especially problematic in applications with a large shaft inertia where it may take minutes for the machine shaft to reach standstill. In such applications, it would be beneficial to resume the machine operation as soon as power is restored.

The goal of this work is to develop a universal restart method that is capable of restarting synchronous reluctance machines (SynRM) driving a high inertia load. In many industrial applications, SynRM is replacing induction machines (IM) and permanent magnet synchronous machines (PMSM), due to the low power density of IM and the high cost of PMSM. In addition, in many applications that high dynamic performance is not required, the machine is controlled in V/Hz mode to ensure easier commissioning by the end-user. As a result, only a few parameters about the machine are known, such as the V-Hz ratio and machine ratings.

The proposed approach borrows concepts from similar work done on induction machines [1-3] and more recently PMSM [4-8]. However, these methods are not suitable for SynRM because (1) there is no permanent magnet and that makes it difficult to use the pulse method used in PMSM method, (2) there is no current conducting in the rotor which makes it impossible to use the searching method used in induction motor and (3) the motor parameter information such as inductance values are not available when using scalar control method.

Another approach to estimate speed and position uses high frequency current injection [9-17]. In general, high frequency injection methods have been proposed for sensorless vector control and estimate the rotor speed and position even at zero speed. However, these methods require a demodulation process and an observer or a state filter which increases the complexity of the restart algorithm. Self-commissioning [18] is another method to determine the machine parameters, but this approach is never used in conjunction with scalar control as it would obviate the commissioning simplicity, considered one of the main benefits of scalar control.

In this paper, we propose an effective restart algorithm for high-inertia drives that use scalar control. The proposed approach minimizes the estimation error and eliminates the need for estimating stator inductance, resulting in the universal SynRM restart algorithm. The remainder of this paper presents the principle of operation of proposed restart algorithm in detail. Experimental results are presented to verify the proposed approach.

II. PROPOSED RESTART METHOD

As above mentioned, the goal of this work is to develop an algorithm suitable for scalar control of SynRM that allows the machine to continue operating after a short power outage. In developing the restart algorithm we have made the following assumptions: (1) during the outage, the drive loses power, but the controller has knowledge of the *v/f* ratio; (2) the controller recognizes the speed command prior to and after the fault and (3) the controller monitors the input power (i.e. recognizes when power was lost and when power was restored). In this section the complete scheme for searching the rotor speed and position is described.

Analyzing the machine equivalent circuit, the resulting equation describing the SynRM machine operation in rotor reference frame can be represented as:

$$\begin{bmatrix} v_d \\ v_q \end{bmatrix} = \begin{bmatrix} R_s + pL_d & -\omega_r L_q \\ \omega_r L_d & R_s + pL_q \end{bmatrix} \begin{bmatrix} i_d \\ i_q \end{bmatrix} \quad (1)$$

978-1-4799-7312-5/18/$31.00 ©2018 IEEE

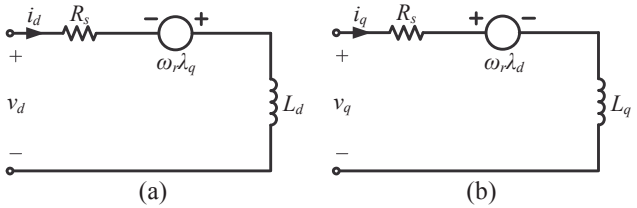

Fig. 1. The equivalent circuit of the SynRM in the rotor reference frame; (a) *d*-axis circuit (b) *q*-axis circuit.

where p denotes the derivative operator, R_s is the stator winding resistance, v_d & v_q are the *d-q* axis stator input voltage, i_d & i_q are the *d-q* axis stator current, L_d & L_q are the *d-q* axis stator inductances and ω_r is the electrical angular frequency of the rotor.

A. Rotor Position Estimation

The concept proposed herein is to excite the machine with active voltage vector (v_1~v_6) and to measure the resulting machine current. To simplify the implementation, v_1 voltage vector is used. v_1 voltage vector aligned with α-axis in stationary reference frame is shown in Fig. 2(a). v_1 vector is applied for t_{pulse} time and repeated every two switching period as shown in Fig. 2(b) while the rotor is rotating with ω_r speed. When applying v_1 voltage vector, it is assumed that the applied voltage pulse time (t_{pulse}) is much smaller than the stator time constants ($\tau_d = L_d/R_s$, $\tau_q = L_q/R_s$). In this case, the stator resistance can be neglected. Assuming the stator resistance R_s is negligible, (1) can be simplified as follows:

$$\begin{bmatrix} v_d \\ v_q \end{bmatrix} = \begin{bmatrix} pL_d & -\omega_r L_q \\ \omega_r L_d & pL_q \end{bmatrix} \begin{bmatrix} i_d \\ i_q \end{bmatrix} \tag{2}$$

v_1 voltage vector can be expressed as $v_a = 2V_{dc}/3$, $v_b = -V_{dc}/3$ and $v_c = -V_{dc}/3$ in stationary reference frame. It can be transformed as $v_d = 2V_{dc}/3 \cdot cos\theta_r$ & $v_q = -2V_{dc}/3 \cdot sin\theta_r$ in rotor reference frame. In here, V_{dc} is the DC-link voltage of voltage source inverter (*VSI*) and θ_r (=$\omega_r t$) is the actual electric rotor angle in stationary reference frame. The resulted *d-q* axis current by v_1 voltage vector can be obtained by solving (2) using *Laplace transform* as:

$$\begin{bmatrix} i_d(t_{pulse}) \\ i_q(t_{pulse}) \end{bmatrix} = \frac{2V_{dc}}{3} \begin{bmatrix} \dfrac{\left(\cos\left(\omega_r t_{pulse}\right)-1\right)\sin\left(\theta_r\right)+\sin\left(\omega_r t_{pulse}\right)\cos\left(\theta_r\right)}{\omega_r L_d} \\ \dfrac{\left(\cos\left(\omega_r t_{pulse}\right)-1\right)\cos\left(\theta_r\right)-\sin\left(\omega_r t_{pulse}\right)\sin\left(\theta_r\right)}{\omega_r L_q} \end{bmatrix} \tag{3}$$

where t_{pulse} is the applied pulse time of v_1 voltage vector. When deriving *d-q* axis current, the initial condition of that current was assumed to be zero as shown in Fig. 2(b). As t_{pulse} is the short time, $\cos(\omega_r t_{pulse})$ and $\sin(\omega_r t_{pulse})$ can be

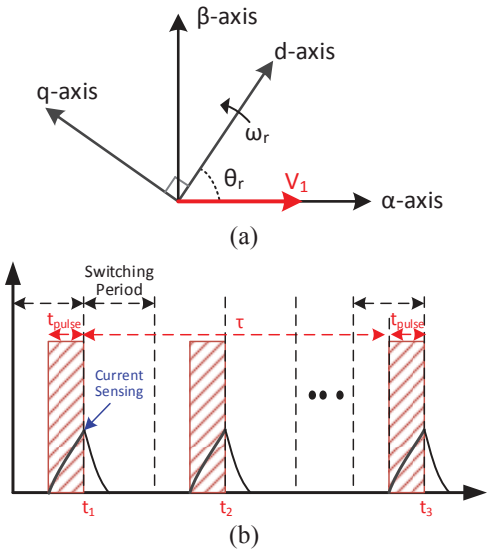

Fig. 2. (a) Applying v_1 voltage vector and (b) v_1 voltage vector pulse and resulting current.

respectively considered as 1 and $\omega_r t_{pulse}$. The *d-q* axis current of (3) can be simplified as:

$$\begin{bmatrix} i_d(t_{pulse}) \\ i_q(t_{pulse}) \end{bmatrix} \approx \frac{2V_{dc}t_{pulse}}{3} \begin{bmatrix} \dfrac{\cos\left(\theta_r\right)}{L_d} \\ -\dfrac{\sin\left(\theta_r\right)}{L_q} \end{bmatrix} \tag{4}$$

The generated torque by the current resulted by v_1 voltage vector is calculated using (4) as:

$$T_e = \frac{3n}{8}\left(\frac{2V_{dc}t_{pulse}}{3}\right)^2\left(\frac{1}{L_d}-\frac{1}{L_q}\right)\sin\left(2\theta_r\right) \tag{5}$$

where n is the machine pole number. The amplitude of the generated torque is small enough to ignore if the voltage vector pulse time is short. The average of the generated torque per one revolution is zero.

From (4), the resulting three phase current can be calculated using inverse Park's transformation as:

$$\begin{aligned} i_a &= \frac{2V_{dc}t_{pulse}}{3}\left(\frac{1}{2}\left(\frac{1}{L_d}+\frac{1}{L_q}\right)+\frac{1}{2}\left(\frac{1}{L_d}-\frac{1}{L_q}\right)\cos\left(2\theta_r\right)\right); \\ i_b &= \frac{2V_{dc}t_{pulse}}{3}\left(-\frac{1}{4}\left(\frac{1}{L_d}+\frac{1}{L_q}\right)+\frac{1}{2}\left(\frac{1}{L_d}-\frac{1}{L_q}\right)\cos\left(2\theta_r-\frac{2\pi}{3}\right)\right); \\ i_c &= \frac{2V_{dc}t_{pulse}}{3}\left(-\frac{1}{4}\left(\frac{1}{L_d}+\frac{1}{L_q}\right)+\frac{1}{2}\left(\frac{1}{L_d}-\frac{1}{L_q}\right)\cos\left(2\theta_r+\frac{2\pi}{3}\right)\right) \end{aligned} \tag{6}$$

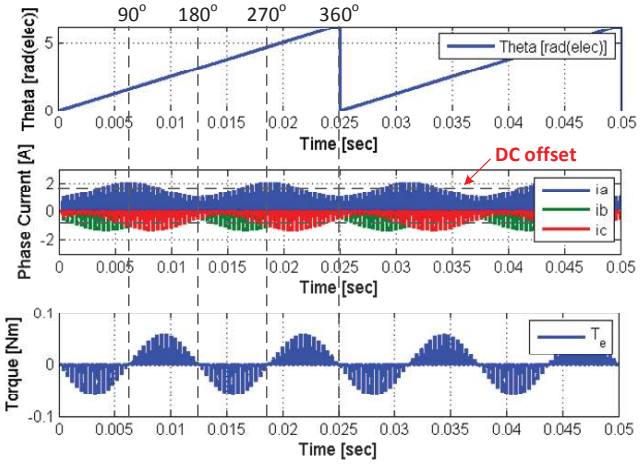

Fig. 3. The resulted phase current and the generated electric torque by v_1 voltage pulse corresponding to the rotor position.

As shown in (6), the three phase current generated by applying v_1 voltage vector consists of two terms. The first term is the *DC*-offset current and second term is the *AC* current oscillation due to the rotor position. The rotor position can be estimated by extracting the *AC* terms from the current of the three phases. It is noticeable that the *AC* current frequency is twice faster than the rotor electric speed. Fig. 3 shows the simulation result when applying v_1 voltage pulse. The machine parameters are listed in Table 1. The rotor speed in the simulation is 1,200 rpm and the applied voltage pulse duty is 50%. The top one is the actual rotor angle, the middle one is the resulted phase current and the bottom one is the generated torque by voltage pulse.

The three phase currents can be used to estimate the rotor speed and position. For that, the *DC*-offset terms of the three phase currents should be eliminated. The *DC*-offset can be obtained by averaging one phase current for several cycles. When v_1 is applied for the estimation, phase *a* current (i_a) has the largest magnitude among the three phase currents and therefore it is selected to guarantee an accurate current sensing.

The *DC*-offset of phase *a* current is expressed as:

$$I_{DC-offset} = \frac{V_{dc} t_{pulse}}{3}\left(\frac{1}{L_d} + \frac{1}{L_q}\right) \tag{7}$$

The three phase *AC* current term (i_{a_AC}, i_{b_AC} and i_{c_AC}) is then calculated by subtracting the *DC*-offset term (7) from the measured phase current as:

$$\begin{aligned} i_{a\_AC} &= A\cos(2\theta_r); \\ i_{b\_AC} &= A\cos\left(2\theta_r - 2\pi/3\right); \\ i_{c\_AC} &= A\cos\left(2\theta_r + 2\pi/3\right) \end{aligned} \tag{8}$$

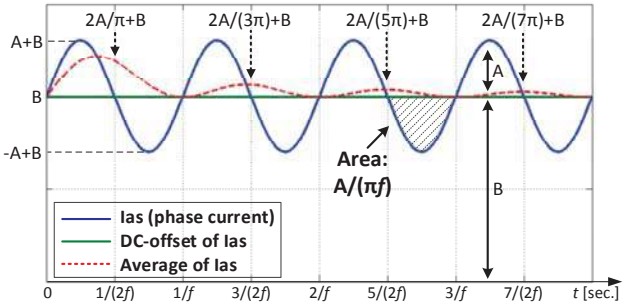

Fig. 4. The DC-offset calculation error by the current averaging method.

In here, A is $V_{dc} \cdot t_{pulse}/3 \cdot (1/L_d - 1/L_q)$. By taking the Clarke transform, α-β current in stationary reference frame can be obtained as:

$$\begin{bmatrix} i_{\alpha\_AC} \\ i_{\beta\_AC} \end{bmatrix} = \begin{bmatrix} 1 & 0 & 0 \\ 0 & \frac{1}{\sqrt{3}} & -\frac{1}{\sqrt{3}} \end{bmatrix} \begin{bmatrix} i_{a\_AC} \\ i_{b\_AC} \\ i_{c\_AC} \end{bmatrix} = \begin{bmatrix} A\cos(2\theta_r) \\ A\sin(2\theta_r) \end{bmatrix} \tag{9}$$

Finally, the rotor position can be estimated by using the following equation.

$$\theta_{est} = \frac{1}{2} tan^{-1}\left(i_{\beta\_AC} / i_{\alpha\_AC}\right) \tag{10}$$

Where, θ_{est} is the estimated electric rotor angle.

The following subsection will investigate the error of the *DC*-offset term obtained by averaging i_a current. The *DC*-offset estimation error is determined by the averaging time, the *AC* amplitude and the *DC*-offset of i_a current. Fig. 4 shows the *DC*-offset obtained at every half period of the current while averaging the i_a current.

In Fig. 4, f is the frequency of phase current, A and B are the *AC* amplitude and the *DC*-offset of i_a current, respectively. The *DC*-offset error at every half period of the phase current can be expressed with the following:

$$\varepsilon = \frac{\Delta I_{DC-offset}}{I_{DC-offset}} = \frac{\int_0^{\frac{n}{2f}} A\sin(\omega t)\,dt}{B} = \frac{A}{B}\frac{1-\cos(n\pi)}{n\pi} \tag{11}$$

In (11), ε is the *DC*-offset calculation error of phase current averaging method and n indicates the order number in every half period of the phase current. Analyzing (11), it is apparent that the *DC*-offset error can be minimized by increasing the n value. As shown in (6), *DC-offset* of phase *a* current (i_a) is always larger than *AC* amplitude. Thus, the minimum ratio of A (*AC* amplitude) and B (*DC-offset*) in (11) can be assumed a number smaller than 1. Then, the required minimum averaging time for the *DC*-offset calculation can be determined as knowing the minimum rotor speed requiring the restart method and the minimum *DC*-offset error (ε). For example, if

the required minimum electric rotor speed is 5*Hz* and the allowed maximum *DC*-offset error is 3%, the minimum averaging time for the *DC*-offset extraction is about 1.0 [sec.] as depicted from (11). The ratio of *A* and *B* was assumed to be 1 which is the worst case.

The theta estimation error caused by *DC*-offset error is investigated with a 3% *DC*-offset error.

$$\begin{aligned} i_{am\_AC} &= i_a - \left(I_{DC-offset} + \Delta I_{DC-offset}\right) = i_{a\_AC} - \varepsilon B; \\ i_{bm\_AC} &= i_b + \frac{\left(I_{DC-offset} + \Delta I_{DC-offset}\right)}{2} = i_{b\_AC} + \frac{\varepsilon}{2} B; \\ i_{cm\_AC} &= i_c + \frac{\left(I_{DC-offset} + \Delta I_{DC-offset}\right)}{2} = i_{c\_AC} + \frac{\varepsilon}{2} B \end{aligned} \quad (12)$$

where $i_{am\text{-}AC}$, $i_{bm\text{-}AC}$ & $i_{cm\text{-}AC}$ are the three phase currents including the error caused by the DC-offset estimation error. For simplification, the ratio of *A* and *B* is assumed to be one which represents the worst case scenario. Then, *B* of (12) can be replaced with *A*. The rotor position is estimated with the three phase *AC* currents by using the following equation.

$$\theta_{est\_m} = \theta_r + \Delta\theta_{error} = \frac{1}{2} tan^{-1}\left(i_{\beta m\_AC} / i_{\alpha m\_AC}\right) \quad (13)$$

Where $\Delta\theta_{error}$ is the theta estimation error term caused by DC-offset error, θ_r is the actual rotor angle. $i_{\alpha m\text{-}AC}$ & $i_{\beta m\text{-}AC}$ is the α-β current in the stationary reference frame obtained from the three phase currents in (12). $\Delta\theta_{error}$ depends on the accuracy of current sensing and *DC*-offset obtained. The effect of current sensing error was investigated in [7, 8]. This analysis assumed that the current sensing error is included in *DC*-offset error. The estimated angle error ($\Delta\theta_{error}$) caused by the 3% *DC*-offset error is shown in Fig. 5. The resulting position estimation error is bounded to be less than 1.7° [deg.]. With this result, the maximum speed estimation error is calcuated in the next section.

B. Rotor Speed Estimation

The next step is to estimate the rotor speed by using two estimated rotor angles (θ_{est}). If the interval time between the two thetas is short enough, the rotor speed can be assumed to be constant. Then, the rotor speed can be estimated by using the two estimated thetas as:

$$\omega_{est} = \frac{\theta_{est2} - \theta_{est1}}{t_{pulse} + \tau} \quad (14)$$

where t_{pulse} is the pulse time in which the v_1 vector is applied to the stator winding, τ is the time between two pulses shown in Fig. 2(b) and ω_{est} is the estimated electrical angular frequency of the rotor. Since the two estimated theta (θ_{est2} & θ_{est1}) might have an error caused by *DC*-offset error, it will also result in a speed estimation error. The estimated speed can be expressed again as:

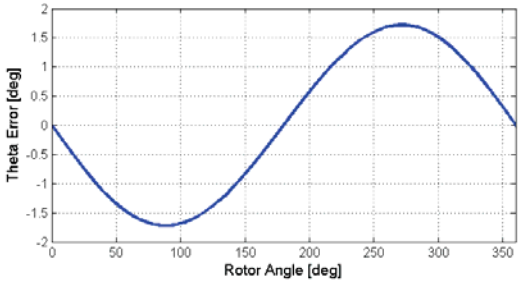

Fig. 5. The angle error caused by the *DC*-offset error.

$$\omega_{est} = \frac{\theta_{est2} - \theta_{est1}}{t_{pulse} + \tau} = \omega_{r\_act} + \frac{2\Delta\theta_{error}}{t_{pulse} + \tau} \quad (15)$$

Where $\Delta\theta_{error}$ is the error of the estimated theta. With longer interval time (τ), the speed estimation can be more precise. However, when choosing the interval time (τ) in Fig. 2(b), the rated speed of the rotor should be considered so that the interval τ is shorter than the time taken for one electrical revolution [6]. If the second theta is estimated after the rotor rotates the electric angle π [*rad.*], the rotating speed of the rotor can be estimated incorrectly.

$$\begin{cases} \omega_{r\_act} = \dfrac{\left(\theta_{r2} + \pi \cdot N\right) - \theta_{r1}}{t_{pulse} + \tau} \\ \omega_{est} = \dfrac{\theta_{est2} - \theta_{est1}}{t_{pulse} + \tau} \end{cases} \quad (16)$$

Where *N* is the rotor rotation number between two theta, ω_{r_act} is an actual speed and ω_{est} is the estimated speed. The estimated speed will be the same as the actual speed when *N* is only zero. Therefore, the following equation should be satisfied to prevent the wrong speed estimation.

$$\theta_{r2} - \theta_{r1} = \omega_r \cdot \left(\tau + t_{pulse}\right) < \pi \quad (17)$$

When calculating the maximum interval time τ, the worst case scenario is assumed which is ω_r is equal to ω_{rated} and t_{pulse} is equal to 100% duty. Then, the difference between the two estimated thetas will not exceed π at any speed condition. ω_{rated} is the maximum speed given on the motor nameplate. For the test motor listed in Table 1, the time interval for the speed estimation is calculated as $40T_{sw}$.

C. Implementation of the Proposed Restart Method

The key performance criteria of the proposed restart method for SynRM motors is to successfully estimate the rotor speed and position with only the motor nameplate parameters and to restart the motors without causing the overcurrent and the braking torque. The proposed complete scheme for estimating the rotor speed and position is shown in Fig. 6.

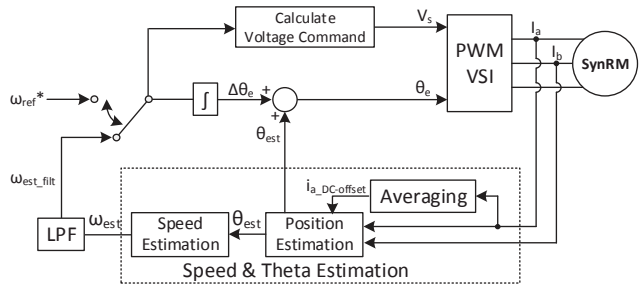

Fig. 6. Complete scheme for estimating the rotor speed and position.

The procedure to implement the restart proposed method is explained in the steps below.

- Step 1 – Apply v_1 voltage vector with the fixed duty and measure the three phase currents (i_{abc}).
- Step 2 – Average the phase current i_a to calculate *DC*-offset term and extract the three phase *AC* current term (i_{abc_AC}).
- Step 3 – Estimate the rotor speed & position.
- Step 4 – If the estimated speed is lower than 20*Hz*, the rotor speed and position should be estimated again with the adjusted new interval time (τ_{new}).
- Step 5 – Compensate the estimated position angle.
- Step 6 – Calculate the command voltage using the rated *v*/*f* ratio.
- Step 7 – Apply the stator voltage to the compensated position angle with the estimated speed.
- Step 8 – Start the stabilizing loop [19] from the next switching cycle with the current feedback.

In step 1, the initial duty of the applied voltage is set as 50%. The magnitude of the phase current generated by v_1 is determined from (4) as:

$$I_{mag} = \frac{2V_{dc}t_{pulse}}{3}\sqrt{\frac{\cos(\theta_r)^2}{L_d^2}+\frac{\sin(\theta_r)^2}{L_q^2}} < \frac{2V_{dc}t_{pulse}}{3L_q} \quad (18)$$

The motor inductance in (18) value is unknown. Therefore, the current magnitude cannot be estimated before applying the v_1 voltage vector to estimate the speed and the position. If the phase current generated by first v_1 voltage pulse exceeds the rated current, the duty is adjusted by knowing the measured current and the rated current.

$$t_{pulse\_new} = \frac{I_{rating}}{I_{measued}} t_{pulse} \quad (19)$$

And then, the estimation procedure is restarted again with new pulse duty.

In step 3, the interval time (τ) in Fig. 2(b) for estimating the speed was determined by the rated speed listed on the motor nameplate.

In step 4, the interval time is adjusted if the initial estimated rotor speed is lower than the 20*Hz* electric rotor speed. If the rotor speed is too slow, the estimated speed in low speed can have a big estimation error as shown in (15). Thus, the new interval time (τ_{new}) is required to accurately estimate the rotor speed in the low speed condition. When the electric rotor speed is slower than 20*Hz* and the maximum theta estimation error is 1.7° [deg.], the speed estimation from (15) might have more than 5% error with the $40T_{sw}$ interval time. In this paper, 5% error is considered as a conservative upper bound on the error [8]. In the experimental result section, the method to adjust the interval time is explained in details along with the test results.

In step 5, the estimated theta is compensated and the compensated theta (θ_{comp}) is given by:

$$\theta_{comp} = \theta_{est} + \frac{\pi}{2} + \omega_{est}T_{sw} \quad (20)$$

The theta (θ_{est}) estimated in the previous step is aligned with the *d*-axis of the motor in the rotor reference frame. By adding π/2 [rad.] to θ_{est}, the compensated theta (θ_{comp}) can be aligned with *q*-axis. The stator voltage is applied to *q* axis to ensure a positive torque at the restart instant. Fig. 7 shows the applied stator voltage vector (v_s) and the resulted current vector (i_s).

In Fig. 7, θ_z is the phase angle of motor impedance, which has a value between 0 and 90°[deg.] because a motor is an inductive load. Then, the *d*-*q* axis current in the rotor reference frame will always be positive, and it will result in a positive electric torque. The torque equation of the SynRM is shown in the following:

$$T_e = \frac{n}{2}\frac{3}{2}\left(L_d - L_q\right)i_d i_q \quad (21)$$

The third term ($\omega_{est}T_{sw}$) in (20) is in order to compensate the current sampling delay. T_{sw} is the PWM switching frequency.

In step 7, the stator voltage frequency is set to the estimated speed frequency. The applied stator voltage magnitude is increased gradually from zero. The voltage increase is stopped when the voltage reaches the rated *v*/*f* value. The purpose is to prevent the inrush current which can be generated by applying step voltages.

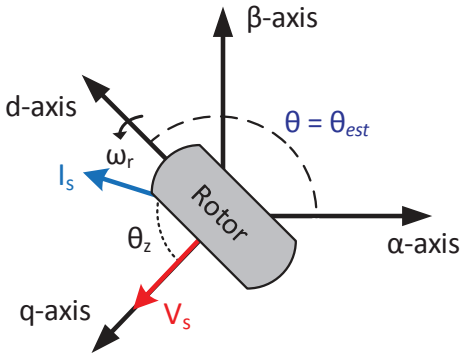

Fig. 7. Vector diagram showing the applied voltage vector at restart moment and the resulting current vector.

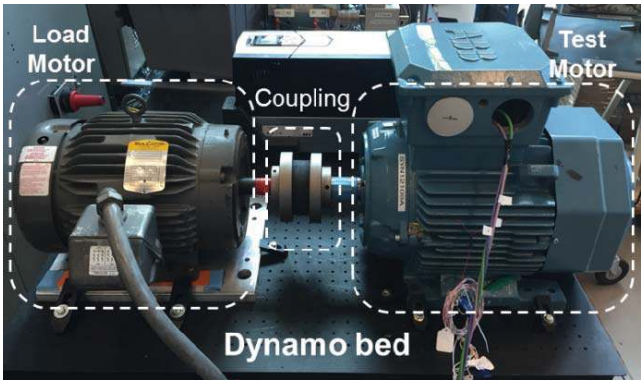

Fig. 8. The dynamo set configuration for the experimental test.

TABLE 1. THE TEST SYNRM MOTOR PARAMETERS.

Parameter	Unit	Symbol	Values
Rated Power	[kW]	P_{out}	18.5
Rated Speed	[rpm]	N_r	1800
Rated Torque	[Nm]	T_e	98
Rated Voltage (line-line)	[V]	V_s	380
Phase Current (rms)	[A]	i_s	43
Pole	-	n	4
Stator Resistor	[Ω]	R_s	0.19
Stator d-axis Inductance	[mH]	L_d	35
Stator q-axis Inductance	[mH]	L_q	17
Inertia	[$Nm/rad{\cdot}s^{-2}$]	J	0.059
Inverter DC Link Voltage	[V]	V_{dc}	540
PWM Switching Period	[μsec]	T_{sw}	200

III. EXPERIMENTAL RESULTS

A set of experiments were conducted to validate performance of the proposed restart method. Fig. 8 shows that the dynamo test bed consisting of the synchronous reluctance motor (SynRM) under test, an induction motor for supplying the load torque. The SynRM motor parameters are given in Table 1. The voltage source inverter (*VSI*) used for driving the test motor is APS-100T120 having the rating of 1200V & 100 A IGBT switches. The selected switching frequency is 5 kHz. V/*f* control method is used and implemented on OPAL-RT platform along with the proposed restart method. To implement our control, only two phase current sensors on the inverter are used. The load motor is fed by another commercial voltage source inverter and the torque & speed were monitored using the analog output of this inverter.

Fig. 9 shows the experimental results of the proposed restart method including the estimated speed and position of the rotor and the stator current when the mechanical rotor speed is 600 and 1500 rpm. The restart tests are implemented using the following steps: the motor is operating at the reference speed. The inverter feeding SynRM motor is stopped intentionally for 1.5 seconds. During that time, the motor speed is reduced by the inertia, the friction and the load condition. After 1.5 seconds, the rotor speed and position estimation is implemented using the proposed method and the motor is again fed by the inverter. Then, the *v*/*f* control is started with

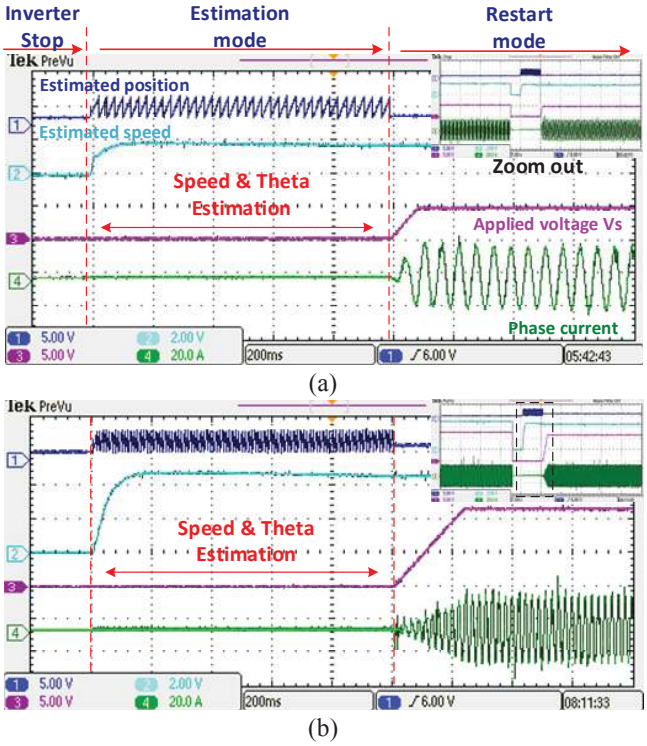

Fig. 9. Restart waveforms of the complete proposed method (a) 600rpm (b) 1,500rpm; CH1: the estimated rotor position, CH2: the estimated speed (600rpm/div.), CH3: the magnitude of stator voltage (100V/div.), CH4: the stator phase current (20A/div.).

the stabilizing loop [19]. The rotor angle (blue line) is estimated with the measured phase current. The speed (cyan line) is estimated with $40T_{sw}$ interval time between two estimated theta. For the position and speed estimation, the estimation process lasts for 1.0 second. The purple line is the applied stator voltage at the restart instant. The command voltage is calculated by using the rated *v*/*f* ratio. The test results of Fig. 9 verify that the performance of the proposed method is good to estimate the rotor speed and position and the restart is implemented without causing any inrush current.

As mentioned before, if the estimated rotor speed is lower than the initially set speed, the interval time between the two pulses for the speed estimation is adjusted in the proposed method. Fig. 10(a) shows the restart result without the interval time adjustment in low rotor speed condition (20*Hz* electric rotor speed). The time interval used for the speed estimation was initially set to $40T_{sw}$. $40T_{sw}$ was calculated by replacing ω_r in (17) with ω_{rated}. In Fig. 10(a), the estimated speed (cyan line) is not constant during the estimation mode. It might cause the position and speed estimation error. The restart is failed due to the overcurrent. The overcurrent is set as 60A considering the machine rated current. On the other hand, Fig. 10(b) shows the test result with the interval time adjustment in low speed condition (5*Hz*). The interval time between two estimated theta is initially set to $40T_{sw}$ and the speed is estimated with these two theta. Based on the estimated speed, if the estimated speed is lower than 20*Hz,* the interval time is

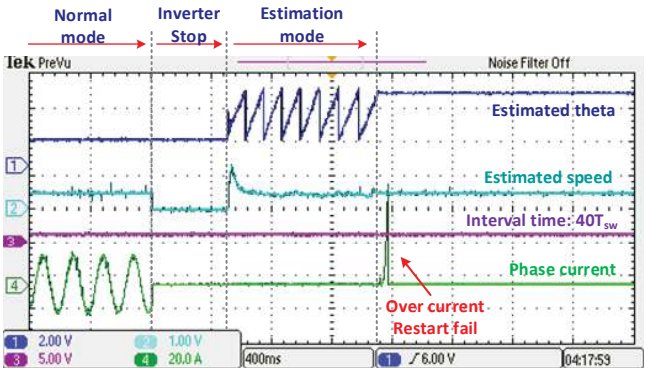

(a)

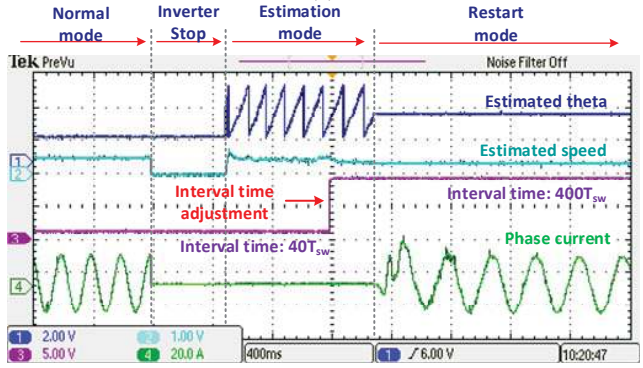

(b)

Fig. 10. The speed estimation in low speed (electric 5Hz speed) (a) without the interval time adjustment (b) with the interval time adjustment; CH1: the estimated theta, CH2: the estimated speed [10Hz/div.], CH3: the interval time (τ) [250T_{sw}/div.], CH4: the actual phase current [20A/div.].

adjusted. The new interval time is calculated from (17), ω_r is replaced with ω_{est} instead of ω_{rated}. The new interval time (τ_{new}) is calculated as:

$$\tau_{new} = 0.9\frac{\pi}{\omega_{est}} \tag{22}$$

In (22), 0.9 is multiplied to give 10% margin because the rotor speed (ω_{est}) estimated with the small interval time might have about 5% error as mentioned before. In the test, the maximum new interval time was limited below 500T_{sw} by considering the switching frequency and the required minimum restart rotor speed. The test result of Fig. 10(b) shows that the interval time (purple line) is automatically changed from 40T_{sw} to 400T_{sw} so that the restart is successful in about 5Hz rotor speed. This experimental test verifies that the SynRM motor can restart successfully even in the low speed condition using this suggested interval time adjustment method.

IV. Conclusions

This paper proposed a novel restart algorithm for SynRM. The proposed method is a universal algorithm that uses only the measured phase current and motor nameplate parameters. In general, the nameplate includes the machine rating information such as the power, the current, the speed and the voltage. It does not include the information such as *d-q* axis stator inductance which the conventional restart methods use. In addition, this method does not require any additional hardware such as speed sensors, phase voltage sensors, DC-link current sensor which are not installed in general purpose drives. This method only requires two phase current information to estimate the speed and position. In addition, a method to minimize the speed estimation error is also presented. The interval time between two pulses used for the speed estimation is automatically adjusted in low speed condition.

This approach is limited to high-inertia SynRM drives because it assumes the rotor is rotating in a near-constant speed during the restart process. However, this limitation is acceptable, as the restart function is only needed for high inertial drives, where reaching standstill may take a relatively long time. To conclude, this proposed method is a universal restart method for SynRM. Experimental results have been conducted to validate the performance of the proposed method.

References

[1] P. Hangwen, L. Springob, J. Holtz, "Improving the start and restart behavior through state recognition of AC drives," *Power Conversion Conference* - Nagaoka 1997., Proceedings of the , vol.2, pp.589,594, 3-6 Aug 1997.

[2] Suzuki, Kentaro, Suzuo Saito, Toshiaki Kudor, Atsushi Tanaka, and Yasuhiro Andoh. "Stability Improvement of V/F Controlled Large Capacity Voltage-Source Inverter Fed Induction Motor," In *Industry Applications Conference*, 2006. 41st IAS Annual Meeting. Conference Record of the 2006 IEEE, vol. 1, pp. 90-95. IEEE, 2006.

[3] Kibok Lee, Sara Ahmed, Srdjan M. Lukic, "Universal Restart Strategy for Scalar (V/f) Controlled Induction Machines," *Industry Applications, IEEE Transactions on*, vol.53, no. 6, pp. 5489-5495, 2017.

[4] Seok-Joo, J. A. N. G., Rostam Dehmoobed Nasrabadi, and Yo Chan Son. "Permanent magnet AC motor systems and control algorithm restart methods," U.S. Patent 8,054,030, issued Nov. 8, 2011.

[5] Takuya Horie, Keiichiro Kondo. "Experimental Study on a Restarting Procedure at Coasting Condition for a Rotational Angle Sensorless PMSM." *IEEJ Journal of Industry Applications*, Vol. 3, no. 2, March 1, 2014.

[6] Toshifumu Y., Shinji W., Keiichiro K., Takashi Y., Shun T., and Shinsuke M., "Starting Procedure of Rotation Sensorless PMSM at Coasting Condition for Railway Vehicle Traction," *Electrical Engineering in Japan*, vol. 169, no. 2, 2009.

[7] Taniguchi, S.; Mochiduki, S.; Yamakawa, T.; Wakao, S.; Kondo, K.; Yoneyama, T., "Starting Procedure of Rotational Sensorless PMSM in the Rotating Condition," *Industry Applications, IEEE Transactions on*, vol.45, no.1, pp.194-202, Jan.-feb. 2009.

[8] Kibok Lee; Sara Ahmed; Srdjan M. Lukic, "Universal Restart Strategy for High-Inertia Scalar-Controlled PMSM Drives," *Industry Applications, IEEE Transactions on*, vol.52, no.5, pp. 4001-4009, 2016.

[9] Lin, T.C.; Zhu, Z.Q., "Sensorless operation capability of surface-mounted permanent magnet machine based on high-frequency signal injection methods," *Industry Applications, IEEE Transactions On*, vol. 51, pp. 2161-2171, 2015.

[10] Lin, T.C.; Zhu, Z.Q., "Novel Sensorless Control Strategy With Injection of High-Frequency Pulsating Carrier Signal Into Stationary Reference Frame," *Industry Applications, IEEE Transactions On*, vol. 50, pp. 2574-2583, 2014.

[11] Sungmin Kim; Jung-Ik Ha; Seung-Ki Sul, "PWM Switching Frequency Signal Injection Sensorless Method in IPMSM," *Industry Applications, IEEE Transactions On*, vol. 48, pp. 1576-1587, 2012.

[12] Murakami, S.; Shiota, T.; Ohto, M.; Ide, K.; Hisatsune, M., "Encoderless Servo Drive With Adequately Designed IPMSM for Pulse-Voltage-Injection-Based Position Detection," *Industry Applications, IEEE Transactions On*, vol. 48, pp. 1922-1930, 2012.

[13] ShihChin Yang; Lorenz, R.D., "Comparison of resistance-based and inductance-based self-sensing controls for surface permanent-magnet machines using high-frequency signal injection," *Industry Applications, IEEE Transactions On*, vol. 48, pp. 977-986, 2012.

[14] T. Tuovinen and M. Hinkkanen, "Adaptive full-order observer with highfrequency signal injection for synchronous reluctance motor drives," *IEEE J. Emerg. Sel. Topics Power Electron.*, vol. 2, no. 2, pp. 181–189, Jun. 2014.

[15] S.-C. Agarlita, I. Boldea, and F. Blaabjerg, "High-frequency-injection assisted 'active flux'-based sensorless vector control of reluctance synchronous motors with experiments from zero speed," *IEEE Trans. Industry Applications*, vol. 48, no. 6, pp. 1931–1939, 2012.

[16] Pin-Chia Pan; Tian-Hua Liu; Udaya K. Madawala, "Adaptive controller with an improved high-frequency injection technique for sensorless synchronous reluctance drive systems," *IET Electric Power Applications*, vol. 10, pp. 240-250, 2016.

[17] T. Tuovinen and M. Hinkkanen, "Signal-Injection-Assisted Full-Order Observer With Parameter Adaptation for Synchronous Reluctance Motor Drives," *IEEE Trans. on Industry Applications*, vol. 50, no. 5, pp. 3392-3402, Sept.-Oct. 2014.

[18] Odhno, S.A.; Giangrande, P.; Bojoi, R.I.; Gerada, C., "Self-Commissioning of Interior Permanent- Magnet Synchronous Motor Drives With High-Frequency Current Injection," *Industry Applications, IEEE Transactions On*, vol. 50, pp. 3295-3303, 2014.

[19] Perera, P.D.C.; Blaabjerg, F.; Pedersen, J.K.; Thogersen, P.; "A sensorless, stable V/f control method for permanent-magnet synchronous motor drives," *Industry Applications, IEEE Transactions on*, Vol. 39, no. 3, pp. 783-791, 2003.